Molecular Imaging
Volume 18: 1-8

DOI: 10.1177/1536012118821032
journals.sagepub.com/home/mix
SAGE

PET Imaging of Hepatocellular Carcinomas: ^{18}F-Fluoropropionic Acid as a Complementary Radiotracer for ^{18}F-Fluorodeoxyglucose

Jing Zhao, MMed[1,2,3], Zhanwen Zhang, MD[3,4,5], Dahong Nie, MD[3,6], Hui Ma, MD[3,4], Gongjun Yuan, MD[3,4], Shu Su, MMed[3,4], Shaoyu Liu, DSc[3,4], Sheng Liu, MD[1,2], and Ganghua Tang, DSc[3,4]

Abstract

Objective: To evaluate the preclinical value of ^{18}F-fluoropropionic acid (^{18}F-FPA) and ^{18}F-fluorodeoxyglucose (^{18}F-FDG) positron emission tomography (PET) for imaging HCCs.

Methods: The ^{18}F-FPA and ^{18}F-FDG uptake patterns in 3 HCC cell lines (Hep3B, HepG2, and SK-Hep1) were assessed in vitro and in vivo. The ^{18}F-FPA uptake mechanism was investigated using inhibition experiments with orlistat and 5-tetradecyloxy-2-furoic acid. The ^{18}F-FPA PET imaging was performed in different tumor animal models and compared with ^{18}F-FDG. We also evaluated the expressions of glucose transporter-1 (GLUT1), fatty acid synthase (FASN), and matrix metalloproteinase-2 (MMP2) in these cell lines.

Results: In vitro experiments showed that the radiotracer uptake patterns were complementary in the HCC cell lines. Orlistat and 5-tetradecyloxy-2-furoic acid decreased the uptake of ^{18}F-FPA. The tumor-to-liver ratio of ^{18}F-FPA was superior to that of ^{18}F-FDG in the SK-Hep1 and HepG2 tumors ($P < .05$). However, in the Hep3B tumors, the tumor-to-liver normalized uptake of ^{18}F-FDG was higher than ^{18}F-FPA ($P < .01$). FASN was highly expressed in cell lines with high ^{18}F-FPA uptake, whereas GLUT1 was highly expressed in cell lines with high ^{18}F-FDG uptake. The ^{18}F-FPA uptake correlated with FASN ($r = 0.89$, $P = .014$) and MMP2 ($r = 0.77$, $P = .002$) expressions.

Conclusions: PET imaging with ^{18}F-FPA combined with ^{18}F-FDG can be an alternative for detecting HCC.

Keywords

hepatocellular carcinoma (HCC), positron emission tomography (PET), ^{18}F-fluoropropionic acid (^{18}F-FPA), ^{18}F-fluorodeoxyglucose (^{18}F-FDG)

[1] Guangdong Provincial Key Laboratory of Malignant Tumor Epigenetics and Gene Regulation, Guangzhou, China
[2] Department of Nuclear Medicine, Sun Yat-sen Memorial Hospital, Sun Yat-sen University, Guangzhou, China
[3] Guangdong Engineering Research Center for Translational Application of Medical Radiopharmaceuticals, The First Affiliated Hospital, Sun Yat-sen University, Guangzhou, China
[4] Department of Nuclear Medicine and Imaging Medicine, The First Affiliated Hospital, Sun Yat-sen University, Guangzhou, China
[5] Department of Nuclear Medicine, The Sixth Affiliated Hospital, Sun Yat-sen University, Guangzhou, China
[6] Department of Radiation Oncology, The First Affiliated Hospital, Sun Yat-sen University, Guangzhou, China

Submitted: 13/08/2018. Revised: 31/10/2018. Accepted: 26/11/2018.

Corresponding Authors:
Ganghua Tang, Department of Nuclear Medicine and Imaging Medicine, Guangdong Engineering Research Center for Translational Application of Medical Radiopharmaceuticals, The First Affiliated Hospital, Sun Yat-sen University, Guangzhou 510080, China.
Email: gtang0224@126.com

Sheng Liu, Guangdong Provincial Key Laboratory of Malignant Tumor Epigenetics and Gene Regulation, Guangzhou 510120, China. Department of Nuclear Medicine, Sun Yat-sen Memorial Hospital, Sun Yat-sen University, Guangzhou 510120, China.
Email: liusheng_gz@126.com

Introduction

Hepatocellular carcinoma (HCC) is the second leading cause of cancer-related death worldwide and therefore a major public health challenge. Early-stage detection and diagnosis of HCC is of vital importance for medical treatment.[1]

Currently, the diagnosis of HCC mainly depends on imaging findings. However, the sensitivity of contrast-enhanced computed tomography (CT) and magnetic resonance imaging (MRI), which are recommended for imaging lesions, is 76% and 61%, respectively.[2] Besides CT and MRI, ^{18}F-fluorodeoxyglucose (^{18}F-FDG) and ^{11}C-acetate positron emission tomography (PET) imaging have demonstrated their capability to detect and stage HCCs. The ^{18}F-FDG PET was introduced for detecting extrahepatic metastases and providing valuable prognostic information in liver transplantation and surgical resection. However, ^{18}F-FDG PET has limited value in diagnosing HCC owing to its low sensitivity.[3] The ^{18}F-FDG is far from being a universal tracer because tumor kinetics may vary and increased glycolysis may not be the preferred kinetic pathway in some tumors. Primary HCC exhibits broad ^{18}F-FDG uptake, thus reducing its sensitivity for tumor detection. The false-negative rate of ^{18}F-FDG PET/CT in HCC is as high as 40% to 50%.[2]

Just as aerobic glycolysis can be a distinguishing attribute of cancer cells, most solid tumors are characterized by a lipogenic phenotype. Hence, fatty acid metabolism—in particular, their biosynthesis—has gained significant attention in the past decade as a biomarker and therapeutic target in multiple cancers.[4-6] ^{11}C-acetate PET, with its higher sensitivity, is an important complement of ^{18}F-FDG. Combining ^{18}F-FDG with ^{11}C-acetate PET/CT has proven useful to clinicians managing patients with HCC.[7]

Although the mechanism of ^{11}C-acetate uptake remains unclear, recent studies have shown that most prostate tumors overexpress fatty acid synthase (FASN), which uses acetate as its substrate for synthesizing short-chain fatty acids, and this could be the reason for the increased ^{11}C-acetate uptake in tumors.[8,9] ^{11}C-acetate has shown promise in diagnosing and staging HCC. However, given the short half-life of carbon-11 (20.4 minutes), the use of ^{11}C-acetate to image tumors and monitor fatty acid synthesis would be limited to institutions with in-house cyclotrons. A potential acetate analog for effectively monitoring fatty acid synthesis could be ^{18}F-fluoroacetate (^{18}F-FAC). However, its drawbacks are its substantial bone uptake and characteristic of radiotracer defluorination that restrict its use.[10] ^{18}F-fluoropropionic acid (^{18}F-FPA)—another important mimic of ^{11}C-acetate—has been proposed as a possible alternative for prostate and breast cancer imaging.[11,12] It has a much higher uptake than acetate does for prostate cancer imaging. Unlike ^{18}F-FAC, ^{18}F-FPA shows low bone uptake and no evidence of defluorination.[12] Our hypothesis was that ^{18}F-FPA would mimic ^{11}C-acetate and hence accumulate in HCCs, thereby allowing tumor delineation on PET. The PET imaging with ^{18}F-FPA combined with ^{18}F-FDG can be an alternative for detecting HCC. Therefore, the aim of this study was to evaluate the preclinical value of ^{18}F-FPA and ^{18}F-FDG PET for imaging HCCs.

Materials and Methods

General

All reagents, unless otherwise specified, were of analytical grade and commercially available. Sep-Pak Light QMA, Sep-Pak Plus C^{18}, Oasis HLB, and SCX cartridges were obtained from Waters Corporation (Milford, Massachusetts). Sep-Pak Light QMA cartridges were preconditioned with 5 mL aqueous $NaHCO_3$ (8.4%) and 10 mL ethanol and water before use. Sep-Pak Plus C^{18} and Oasis HLB cartridges were preconditioned with 10 mL ethanol and water before use. All high-performance liquid chromatography solvents were filtered before use. Radioactivity was measured using a gamma-counter (SN-6105, Shanghai Nuclear Rihuan Photoelectric Instrument, LLC, China).

Cell Culture and Animal Models

All experiments were performed under a protocol approved by the Sun Yat-sen University Institutional Animal Care and Use Committee. SK-Hep1 and Hep3B cell lines were obtained from the Cell Bank of the Chinese Academy of Sciences (Shanghai, China). HepG2 cell line was obtained from the Laboratory Animal Centre of Sun Yat-sen University (Guangzhou, China).

The cells were cultivated in Dulbecco's modified Eagle's medium with a physiologic glucose concentration (1.0 g/L) containing 10% fetal calf serum at 37°C in a humidified atmosphere of 5% CO_2 and 95% air. The medium was routinely renewed 3 times a week. Exponentially growing cells were used for the experiments. BALB/c nude mice were obtained from the Laboratory Animal Centre of Sun Yat-sen University. The mice were kept in sterile surroundings with a standardized light/dark cycle and access to food and water ad libitum. The mice were 6 to 8 weeks old when used for the experiments. Subcutaneous tumors were produced in the BALB/c nude mice (16-20 g) via subcutaneous injection of 5×10^6 tumor cells in a 100-μL volume comprising 50 μL of the cell culture medium and 50 μL of Matrigel (BD Biosciences, New Jersey) on the forelimb of the mice. The ^{18}F-FPA and ^{18}F-FDG PET/CT were performed when the tumors were 5 to 8 mm in diameter.

Radiosynthesis

No-carrier-added ^{18}F-fluoride ion was obtained through the nuclear reaction ^{18}O(p, n)^{18}F by irradiating more than 95% ^{18}O-enriched water targeted with 10-MeV protons using a Cyclone 10/5 cyclotron (IBA Technologies, Belgium).

The ^{18}F-FDG was synthesized automatically with a conventional module used in our clinical work and had a radiochemical purity of more than 95%. Automated radiosynthesis of ^{18}F-FPA was based on previously described methodology,[13] and the final radiochemical yield was around 45% (2%; $n = 20$) with a radiochemical purity of more than 95%.

Cell Uptake Experiment

The Hep3B, HepG2, and SK-Hep1 HCC cells ($\sim 1 \times 10^7$) were seeded on 24-well plates overnight and incubated for 24 hours in a humidified 5% CO_2 environment, at which time greater than 90% confluence was reached. Approximately 0.74 MBq ^{18}F-FPA or ^{18}F-FDG was then added to the wells and incubated at 37°C for 60 minutes. At the end of incubation, the cells were washed 2 times with phosphate-buffered saline (PBS) to remove free tracers and then lysed in 1% NaOH (500 μL for 20 minutes) and transferred to test tubes. Cellular tracer uptake was counted using the gamma-counter. The amount of radioactivity in the cells was normalized by the dose administered per well.

In Vitro Competitive Inhibition Study

The Hep3B, HepG2, and SK-Hep1 HCC cells were seeded on 24-well plates and incubated for 24 hours. After a 30-minute incubation period with orlistat or 5-tetradecyloxy-2-furoic acid (TOFA; run in a concentration series from 0 to 400 μM), ^{18}F-FPA were added at doses of approximately 0.74 MBq/well and the cells were incubated for 20 minutes. The cells were then washed 2 times with PBS, lysed in 1% NaOH (500 μL for 20 minutes), transferred to test tubes, and counted for ^{18}F activity in the gamma-counter. The amount of radioactivity in the cells was normalized by the dose administered per well. This experiment was repeated in triplicate, averaged on different days.

PET/CT Studies and Image Analysis

The PET/CT images were acquired using an Albira small-animal PET/CT scanner (Bruker, Germany) after a bolus injection into the tumor-bearing mice. There were 3 group mice bearing different cell lines. Each group has 3 to 5 mice. The mice were anesthetized using 2% pentobarbital sodium (40 mg/kg) and positioned prone on the scanning table. The mice were kept fasting for at least 4 hours and then ^{18}F-FPA was administered via the tail vein at a dose of 3.70 to 4.44 MBq in 0.2 mL of saline. On the following day, the mice were injected with ^{18}F-FDG in the same condition. Image data were acquired for 20 minutes after 60 minutes of the injection. Static PET scans were acquired and the CT scan was used for attenuation correction and localization of the lesion site. The Albira PET system and PMOD version 3.7 software (PMOD Technologies, Switzerland) were used for imaging construction and for drawing the regions of interest over the tumors and organs. Tumor radioactivity was normalized to that of the whole body to obtain the normalized uptake value to permit comparison of the data obtained.

Histopathology

The excised tumors were fixed in 4% paraformaldehyde and embedded in paraffin. Five-micron sections of each tissue were stained with hematoxylin and eosin, and the tumors were examined.

Immunofluorescence and Western Blotting

Immunofluorescence. The sections were fixed in 4% formaldehyde (10 minutes) and then incubated in 1% bovine serum albumin/10% normal goat serum/0.3 M glycine in 0.1% PBS–Tween for 1 hour to permeabilize the cells and block nonspecific protein–protein interactions. The cells were then incubated with glucose transporter-1 (GLUT1) and FASN antibodies (AB652/AB22759, 1:250/1:100, Abcam, UK) overnight at 4°C. The secondary antibody (red) was CY3 goat anti-rabbit (GB21303, Servicebio, China) immunoglobulin G used at a 1/300 dilution for 50 minutes. Fluorescein isothiocyanate (GB22303, Servicebio) was used at a 1/200 dilution for 50 minutes. 4′,6-Diamidino-2-phenylindole (G1012, Servicebio) was used to stain the cell nuclei (blue) at a concentration of 1.43 μM.

Western blot analysis. The GLUT1, FASN, and matrix metalloproteinase-2 (MMP2) expression levels were measured using Western blot analysis. Samples were lysed with a lysis buffer containing a protease inhibitor cocktail (G2006, Servicebio), and the protein concentrations were determined using a protein assay kit (G2006, Servicebio). Sodium dodecyl sulfate-polyacrylamide gel electrophoresis was performed with 20 μg of protein in each sample using 4% to 15% Mini Protean TGX precast gels (Servicebio). The following primary antibodies were used: anti-GLUT1 (AB652, 1:1000, Abcam), anti-FASN (AB22759, 1:1000, Abcam), and anti-MMP2 (GB11130, 1:1000, Servicebio). The bands were detected using a Western blotting detection system (Epson, Japan) and band intensity was calculated via densitometry using AlphaEaseFC (Alpha Innotech, USA).

Statistical analysis. Quantitative data were expressed as means (standard deviation). Statistical analysis was performed using PASW Statistics for Windows, version 18.0 (SPSS Inc, Chicago, Illinois). An independent-sample t test was used for comparing the differences between the uptake of ^{18}F-FPA and ^{18}F-FDG. Analysis of variance was used for comparing between the HCC cell lines. The correlation between the results of Western blotting and radiotracer uptake was analyzed using linear regression analysis. P values <.05 were considered statistically significant.

Results

In Vitro Studies

The HCC cell lines showed significantly varied ^{18}F-FDG and ^{18}F-FPA uptakes (Figure 1A and). After incubation for 60 minutes, ^{18}F-FPA uptake in the Hep3B, HepG2, and SK-Hep1 cells reached 0.0024% (0.0003%), 0.0035% (0.0001%), and 0.0039% (0.0007%) radioactivity per microgram of protein, respectively ($F = 6.909$, $P = .028$). In contrast, ^{18}F-FDG uptake at the same point in the Hep3B, HepG2, and SK-Hep1 cells reached 0.0082% (0.0016%), 0.0067% (0.0022%),

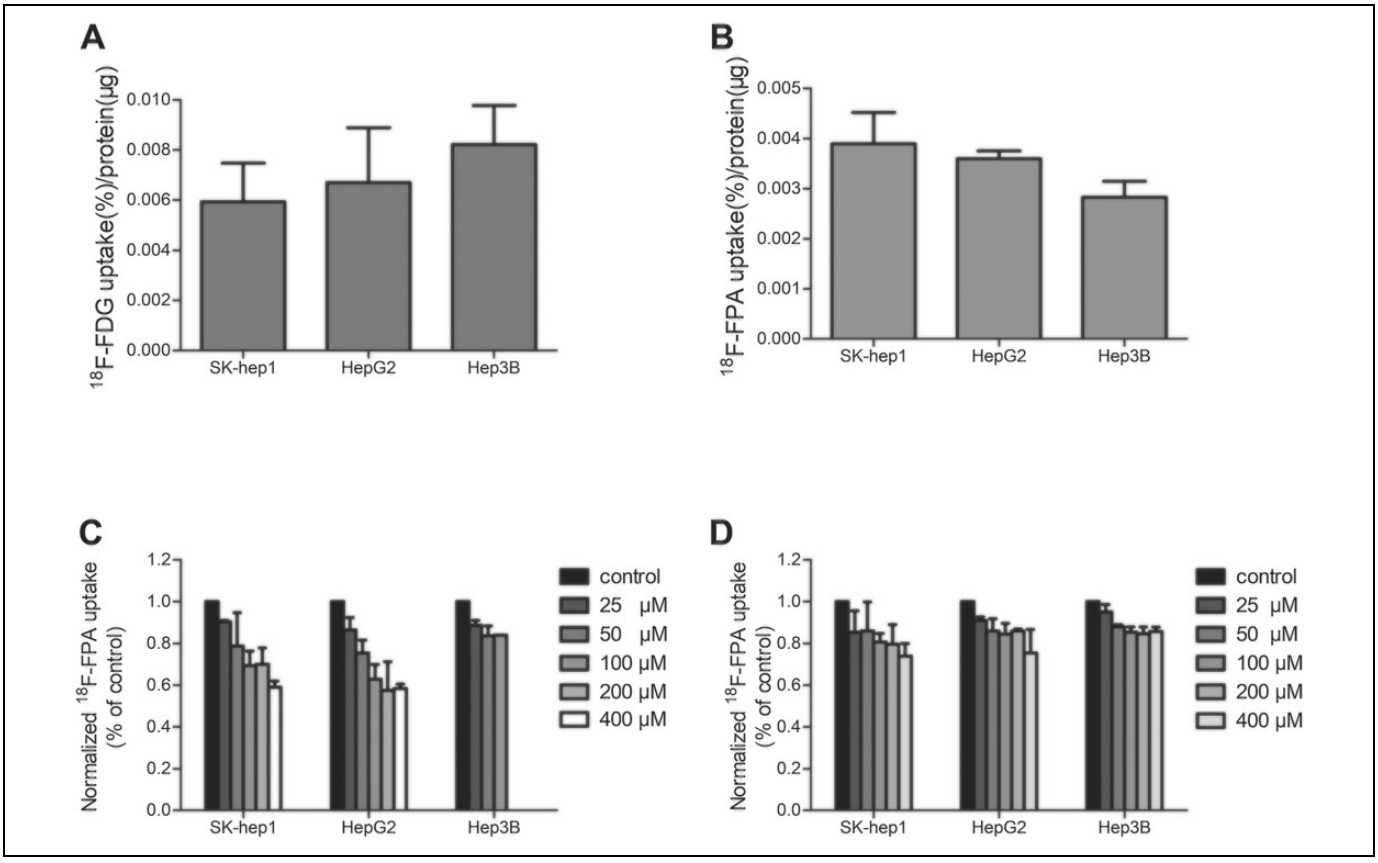

Figure 1. Patterns of ^{18}F-fluoropropionic acid (^{18}F-FPA) or ^{18}F-fluorodeoxyglucose (^{18}F-FDG) uptake in hepatocellular carcinoma (HCC) cell lines and the inhibitory effects of orlistat and 5-tetradecyloxy-2-furoic acid (TOFA) on ^{18}F-FPA uptake. A, ^{18}F-FPA uptake is measured at 60 minutes in the HCC cell lines, SK-Hep1, HepG2, and Hep3B. B, ^{18}F-FDG uptake is measured at 60 minutes in these HCC cell lines. C, ^{18}F-FPA uptake in the presence of orlistat. D, ^{18}F-FPA uptake in the presence of TOFA. Data are mean (standard deviation).

and 0.0059% (0.0016%) radioactivity per microgram of protein, respectively ($F = 1.394$, $P = .330$).

In SK-Hep1, HepG2, and Hep3B cells, the uptake of ^{18}F-FPA was inhibited 41.0% (3.0%), 41.6% (2.0%), and 34.7% (8.2%), respectively, by orilistat at 400 μM concentration (Figure 1C). The TOFA revealed a 26.0% (6.0%), 22.0% (2.8%), and 14.3% (2.1%) maximum decrease in ^{18}F-FPA uptake in SK-Hep1, HepG2, and Hep3B, respectively.

Comparison of ^{18}F-FPA and ^{18}F-FDG for Tumor Detection

The PET/CT images were acquired 60 minutes after the injection (Figure 2). High tumor uptake was detected by PET/CT for ^{18}F-FPA or ^{18}F-FDG in HCCs, which showed a similar tendency to that seen in the in vitro study. In static ^{18}F-FPA scans, the tumors were clearly visible with high contrast to the contralateral background within the HepG2 and SK-Hep1 tumor animal models, whereas tumor-associated radioactivity with ^{18}F-FDG was not visible above the background in static scans. For HepG2 and SK-Hep1 tumors, the tumor-to-liver normalized uptakes were 1.40 (0.02) and 1.63 (0.26), respectively, at 60 minutes for ^{18}F-FPA, whereas they were 1.21 (0.08) and 1.09 (0.21) for ^{18}F-FDG ($t = 2.826$, $P = .048$; $t = 4.055$, $P = .047$). In contrast, for Hep3B tumors, the tumor-to-liver normalized uptake was 2.03 (0.25) at 60 minutes for ^{18}F-FDG, whereas it was 0.93 (0.15) for ^{18}F-FPA ($t = 6.472$, $P = .006$).

Consistent with the tendency seen in other in vitro studies, tumor radioactivity was comparable to that of human HCC tumors. The 2 radiotracer uptake patterns seemed to complement each other in HCC tumors. For ^{18}F-FPA, the SK-Hep1 tumors showed 1.2-fold higher tumor-to-liver ratios than did the HepG2 tumors and 1.8-fold higher ratios than did the Hep3B tumor. Conversely, the tumor-to-liver ratios of ^{18}F-FDG in Hep3B tumors were higher than those in HepG2 (1.7-fold) and SK-Hep1 (1.9-fold) tumors.

Histopathological Finding of Tumors

A large number of heterotype cells can be seen in tumor tissues, confirming the success of tumor model making (Figure 2C).

Immunofluorescence Staining

Previous studies indicated that not all HCC tumor samples showed elevated FASN expression.[14] Notably, we found that the SK-Hep1 and HepG2 tumors showed more intense staining

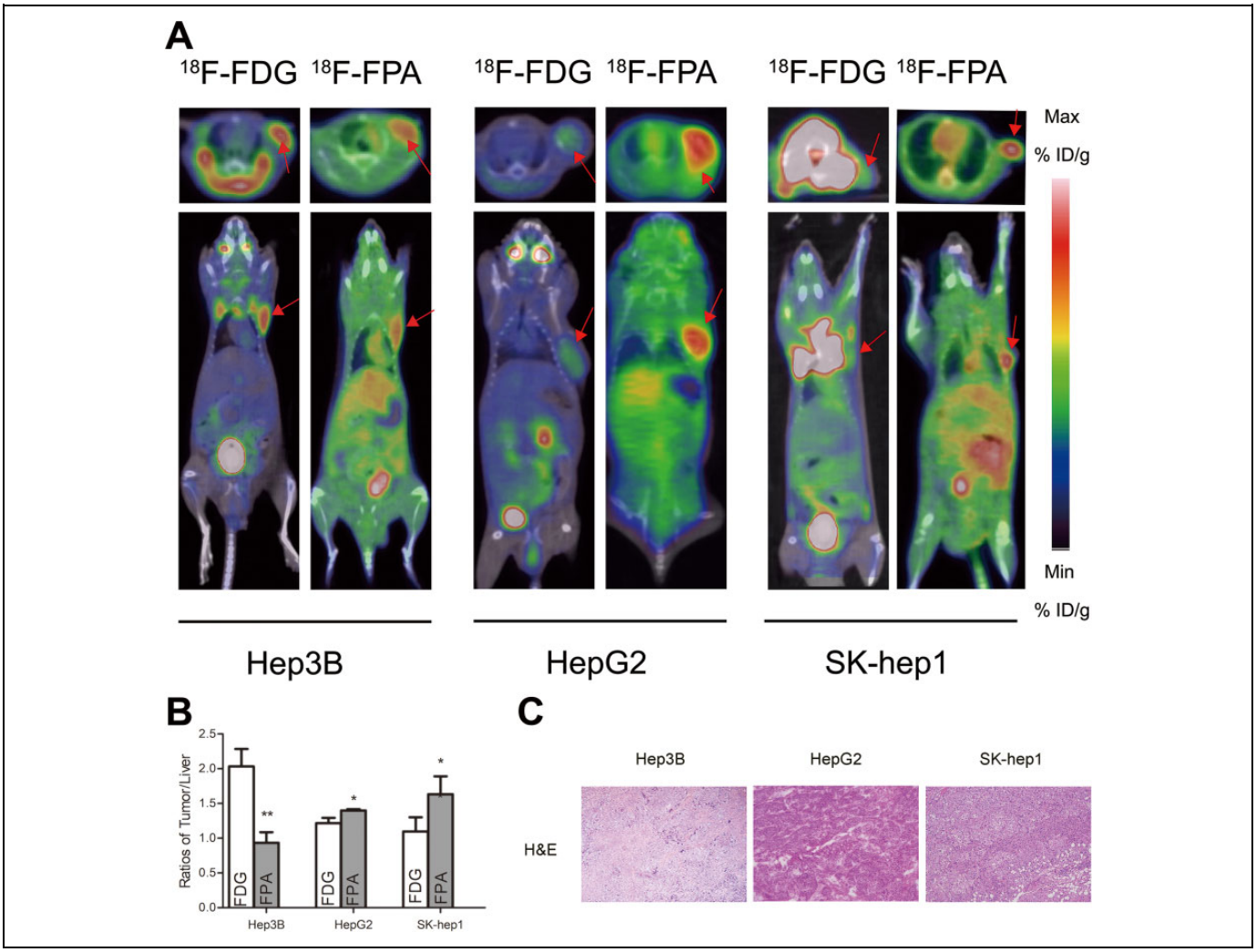

Figure 2. Small animal positron-emission tomography/computed tomography (PET/CT) imaging, quantification, and immunohistochemistry. A, PET/CT images of different hepatocellular carcinoma (HCC) cell-bearing mice (Hep3B, HepG2, and SK-Hep1) acquired as static scans at 60 minutes after the injection of ^{18}F-fluoropropionic acid (^{18}F-FPA) or ^{18}F-fluorodeoxyglucose (^{18}F-FDG; the red arrows indicate the tumor). B, Normalized tumor-to-liver radioactivity at 60 minutes after the injection of ^{18}F-FPA or ^{18}F-FDG (n = 3-5 mice per group; bars represent means [standard deviation]). * $P < .05$, ** $P < .01$, *** $P < .001$. C, Histopathological examination using hematoxylin and eosin staining (H&E staining) in HCC tumor samples. Original magnification: ×100. NS indicates not statistically significant.

of FASN than did the Hep3B tumors, as shown in Figure 3. In contrast, GLUT1 staining was weaker in the SK-Hep1 tumors than in the Hep3B tumors. The results were further confirmed by Western blotting (Figure 4A).

Western Blot and Linear Regression Analysis

Western blot analysis was performed to evaluate the expression of GLUT1, FASN, and MMP2 in SK-Hep1, HepG2, and Hep3B tumors (Figure 4A). Consistent with the results of immunofluorescence staining, the expression of FASN was greater in SK-Hep1 and HepG2 tumors than in Hep3B tumors. Hep3B tumors showed more GLUT1 expression than did the other tumors. A correlation was found between ^{18}F-FPA uptake and FASN expression ($r = 0.89$, $P = .014$) and MMP2 expression ($r = 0.77$, $P = .002$), as shown in Figure 4B and C.

Discussion

The combined ^{11}C-acetate and ^{18}F-FDG PET/CT protocol has been used to evaluate patients with HCC or suspicious liver masses. The results suggest that it has a mutual complementary advantage.[15] Despite the success of ^{11}C-acetate for diagnosing HCC tumors, the short half-life of ^{11}C limits its use as a routine PET agent. In contrast, ^{18}F-labeled tracers are advantageous because of their relatively longer half-life (2 hours) which does not necessitate an onsite cyclotron. One point to note is that ^{18}F-FPA had much higher uptake than ^{14}C-acetate in CWR22rv1 tumors, and the uptake ratio of tumor to some organs was more favorable for ^{18}F-FPA than for ^{14}C-acetate.[12] This study investigated the potential of combining ^{18}F-FDG and ^{18}F-FPA PET as a diagnostic approach for HCCs. The interesting observation is that these 2 tracers are probably

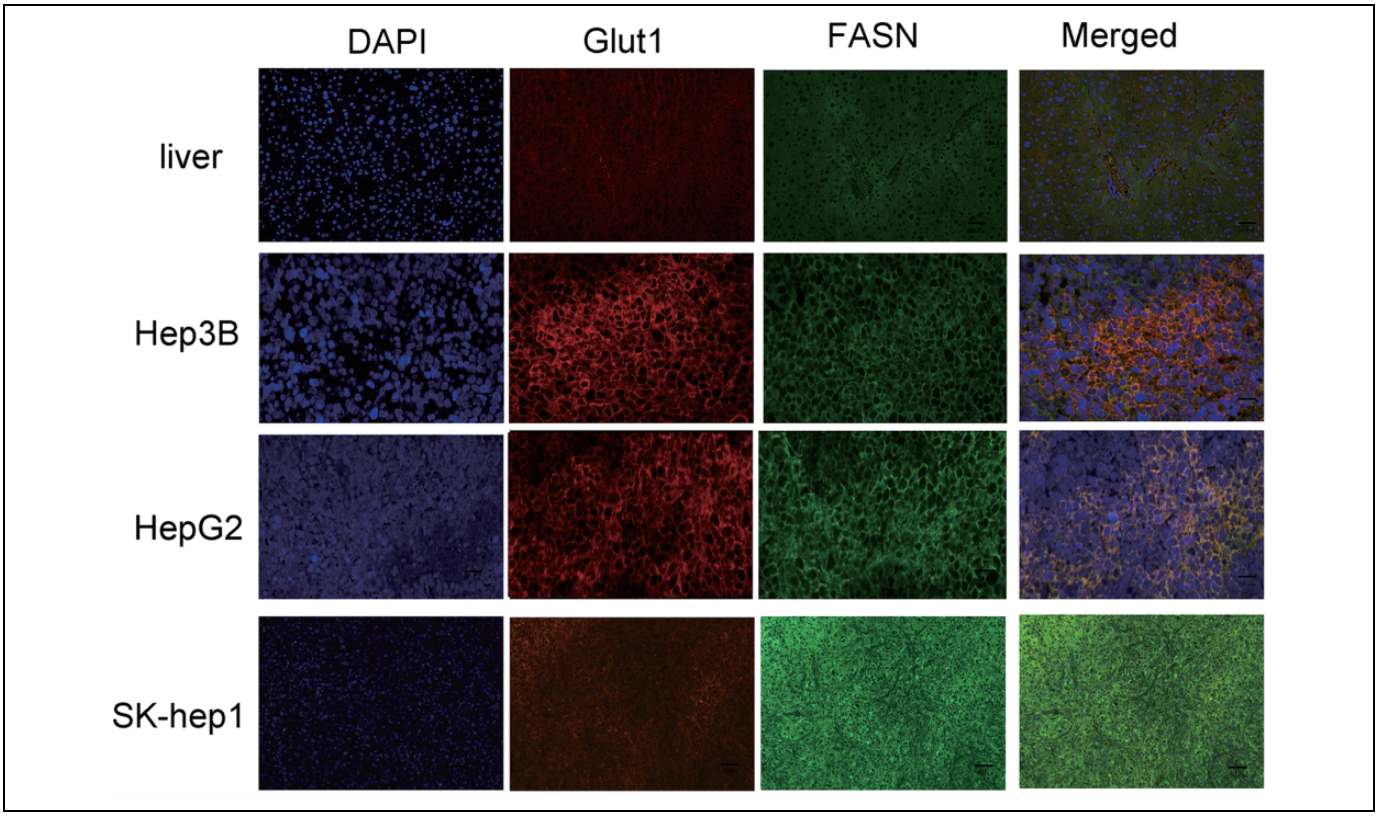

Figure 3. Representative immunofluorescence (IF) staining of the Hep3B, HepG2, and SK-Hep1 tumors. DAPI (blue), anti-GLUT1 (red), and anti-FASN (green) staining. Magnification: ×200. DAPI indicates 4′,6-diamidino-2-phenylindole; GLUT1, glucose transporter-1; FASN, fatty acid synthase.

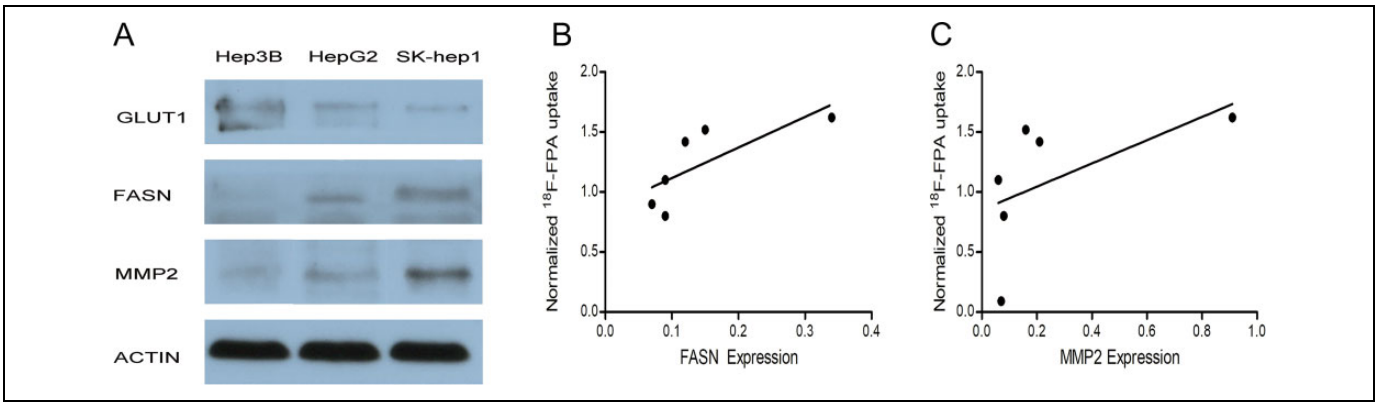

Figure 4. Western blot and linear regression analysis. A, Western blot analysis of GLUT1, FASN, and MMP2 expression in Hep3B, HepG2, and SK-Hep1 tumors. Actin antibody is the loading control. B, Linear regression analysis between FASN expression and tumor-to-liver ratios for ^{18}F-fluoropropionic acid (^{18}F-FPA) positron-emission tomography/computed tomography (PET/CT) in hepatocellular carcinomas (HCCs). C, Linear regression analysis between MMP2 expression and the tumor-to-liver ratios for ^{18}F-FPA PET/CT in HCCs. GLUT1 indicates glucose transporter-1; FASN, fatty acid synthase; MMP2, matrix metalloproteinase-2.

complementary to each other in detecting HCCs. Their combination would increase the sensitivity of PET/CT. When HCCs show a lower ID%/g for ^{18}F-FDG, the uptake of ^{18}F-FPA appears to be quite high. The ^{18}F-FPA shows promise for detecting tumors, which highly express FASN when ^{18}F-FDG PET/CT fails to detect HCCs, and provides more information about metastatic potentials which would be helpful for customizing tumor treatment in clinical practice.

The ^{18}F-FDG PET has been particularly effective in characterizing malignancies that have a glycolytic phenotype. However, various tumors, including primary HCCs, renal cell carcinomas, and certain types of lymphoma, are not easily

visualized by ^{18}F-FDG PET. This is mainly because these tumors are generally not highly glycolytic and thus do not readily accumulate FDG. Although the experimental quantity was small, it is interesting to find that ^{18}F-FDG uptake in the HCC cell lines were so different and that the uptake eventually reflected the differences in the expression of GLUT1 that plays a vital role in ^{18}F-FDG uptake.

Fatty acid synthesis occupies a central role in regulating multiple dynamic processes in tumor cells. Cancer cells often require fatty acids to maintain proliferation and viability. The ubiquitous requirement for fatty acid synthesis in cancer cells provides an opportunity to harness this trait using modern PET/CT technology. ^{11}C-acetate has high sensitivity and specificity as a radiotracer complementary to ^{18}F-FDG in PET imaging of HCCs and evaluation of other liver masses. A high PET signal in tumors is often associated with increased expression of FASN and increased de novo lipogenesis in tumor tissues.[16] The ^{18}F-FPA, as a mimic of ^{11}C-acetate, has the potential to detect HCCs, and its connection to tumor pathobiology is discussed in our work. Generally, sodium, potassium, and calcium salts of propionic acid are extensively used as food additives. Metabolic studies have indicated that propionate can be used as a precursor for synthesizing fatty acids, glycogen, amino acids, and so on depending on the species.[17] Propionic acid metabolism begins with its conversion to propionyl-CoA catalyzed by mitochondrial propionyl-CoA-synthetases, as the first common step in the metabolism of fatty acids.[18,19] Some studies have reported that propionate replaces acetate as a favored energy substrate in the heart and tumor cells,[20] and the net utilization of acetate by rat hepatocytes could be impaired by propionate.[21] Our study showed that ^{18}F-FPA is partly involved in de novo lipogenesis and may be another small fatty acid PET imaging agent for HCC. The uptake of ^{18}F-FPA was inhibited to varying degrees in the presence of inhibitors of fatty acid synthesis. These data demonstrated that orlistat and TOFA are more effective in HCC cell lines with high ^{18}F-FPA uptake. Orlistat, an antiobesity drug having very low oral bioavailability, has been approved by the US Food and Drug Administration. The activity of orlistat has been attributed to its FASN-blocking potential. It shows promising inhibitory effect on cell proliferation as well as tumor growth in prostate and breast cancer cells.[22] The finding that orlistat could reduce the uptake of ^{18}F-FPA by up to 42.7% in HCC cells indicated the important role of FASN in ^{18}F-FPA uptake. In accordance with the results of immunofluorescence and proteomic analyses, the expression of FASN was in the same order which may help explain the mechanism of ^{18}F-FPA uptake. In addition to FASN, other enzymes in the fatty acid synthesis pathway are commonly overexpressed in cancer. For example, the protein expression of acetyl-CoA-carboxylase (ACC), the rate-limiting enzyme upstream of FASN, has been shown to be upregulated in numerous tumor types.[23] The TOFA, a lipophilic fatty acid mimic that targets the carboxyltransferase activity of ACC, inhibited fatty acid synthesis in hepatocytes, rat liver homogenates, and male rat liver by reducing endogenous fatty acids that form part of the phospholipid composition of cell membranes.[24] In terms of ^{18}F-FPA, the treatment of HCC cell lines with TOFA blocked the uptake of this radiotracer even though its inhibition was less effective than that of orlistat. Given that ^{18}F-FPA incorporation into tumor cells directly correlates with the extent of fatty acid synthesis, the efficacy of treatment molecules that regulate the activity of fatty acid synthesis could easily be monitored using ^{18}F-FPA PET. The present data suggested that ^{18}F-FPA uptake is associated with increased expression of FASN and increased de novo lipogenesis in tumor tissues. Recent findings suggest that FASN might play a more or less pronounced role depending of the etiology associated with HCC development, at least in the early phases of hepatocarcinogenesis.[19,25] Early upregulation of FASN in precursor lesions might represent an obligatory metabolic acquisition in response to the microenvironment of preinvasive lesions (ie, poor oxygenation and high acidity, and/or the lack of nutrients), which continue to occur in the invasive and/or metastatic stages. The FASN can work as a previously unrecognized metabolic intermediate of oncogenesis linking energy, anabolism, and malignant transformation.[26] Thus, we inferred that the FASN-related uptake of ^{18}F-FPA may provide more biological information regarding the development and progression of HCCs. The invasion and metastasis of liver cancer is a complex process in which the dissolution of the extracellular matrix plays an important role. The MMP2 is capable of degrading the majority of components of the extracellular matrix and is regarded to closely correlate with tumor invasion and metastasis.[27] In our study, MMP2 overexpression correlated well with ^{18}F-FPA uptake, and we hypothesized that ^{18}F-FPA can provide more information about the metastatic potential of HCC cell lines.

Some limitations of this study should be considered before drawing any conclusions. In vitro experiments, the uptake of ^{18}F-FDG is much higher than that of ^{18}F-FPA in HCC cell lines, suggesting that there are some differences in uptake capacity between tumor cells and tumor tissues. The differences in the microenvironment and other possible related factors should be taken into account. Additional studies are ongoing in more animals, and clinical studies are needed to confirm the relationship between the 2 tracers.

Conclusions

The patterns of ^{18}F-FPA and ^{18}F-FDG uptake seemed complementary to each other in HCC cell lines. The ^{18}F-FPA can be an alternative radiotracer for detecting HCCs with low ^{18}F-FDG uptake. The FASN-related uptake of ^{18}F-FPA may provide more biological information regarding HCC progression. The PET imaging with ^{18}F-FPA combined with ^{18}F-FDG can be an alternative for detecting HCC. Further studies are required to evaluate the possibility of applying this technique in clinical trials.

Authors' Note

Jing Zhao and Zhanwen Zhang contributed equally to this work.

Declaration of Conflicting Interests

The author(s) declared no potential conflicts of interest with respect to the research, authorship, and/or publication of this article.

Funding

The author(s) disclosed receipt of the following financial support for the research, authorship, and/or publication of this article: This work was supported in part by the National Natural Science Foundation of China (No. 81371584, No. 81671719), the Science and Technology Foundation of Guangdong Province (No. 2016B090920087, No. 2013B021800264), and the Science and Technology Planning Project Foundation of Guangzhou (No. 20160402016, No. 201510010145).

References

1. Gomes MA, Priolli DG, Tralhao JG, Botelho MF. Hepatocellular carcinoma: epidemiology, biology, diagnosis, and therapies. *Rev Assoc Med Bras (1992)*. 2013;59(5):514–524. doi:10.1016/j.ramb.2013.03.005.
2. Haug AR. Imaging of primary liver tumors with positron-emission tomography. *Quarter J Nucl Med Mol Imaging*. 2017; 61(3):292–300. doi:10.23736/s1824-4785.17.02994-6.
3. Asman Y, Evenson AR, Even-Sapir E, Shibolet O. [18F]fludeoxyglucose positron emission tomography and computed tomography as a prognostic tool before liver transplantation, resection, and loco-ablative therapies for hepatocellular carcinoma. *Liver Transplant*. 2015;21(5):572–580. doi:10.1002/lt.24083.
4. Jain A, Mathur A, Pandey U, Sarma HD, Dash A. (68)Ga labeled fatty acids for cardiac metabolic imaging: Influence of different bifunctional chelators. *Bioorg Med Chem Lett*. 2016;26(23): 5785–5791. doi:10.1016/j.bmcl.2016.10.048.
5. Hopperton KE, Duncan RE, Bazinet RP, Archer MC. Fatty acid synthase plays a role in cancer metabolism beyond providing fatty acids for phospholipid synthesis or sustaining elevations in glycolytic activity. *Exp Cell Res*. 2014;320(2):302–310. doi:10.1016/j.yexcr.2013.10.016.
6. Cai Z, Mason NS, Anderson CJ, Edwards WB. Synthesis and preliminary evaluation of an (1)(8)F-labeled oleic acid analog for PET imaging of fatty acid uptake and metabolism. *Nucl Med Biol*. 2016;43(1):108–115. doi:10.1016/j.nucmedbio.2015.08.005.
7. Dunphy MP, Lewis JS. Radiopharmaceuticals in preclinical and clinical development for monitoring of therapy with PET. *J Nucl Med*. 2009;50(suppl 1):106s–121s. doi:10.2967/jnumed.108.057281.
8. Deford-Watts LM, Mintz A, Kridel SJ. The potential of (1)(1)C-acetate PET for monitoring the fatty acid synthesis pathway in tumors. *Curr Pharm Biotechnol*. 2013;14(3):300–312.
9. Grassi I, Nanni C, Allegri V, et al. The clinical use of PET with (11)C-acetate. *Am J Nucl Med Mol Imaging*. 2012;2(1):33–47.
10. Ponde DE, Dence CS, Oyama N, et al. ^{18}F-fluoroacetate: a potential acetate analog for prostate tumor imaging – in vivo evaluation of ^{18}F-fluoroacetate versus ^{11}C-acetate. *J Nucl Med*. 2007;48(3): 420–428.
11. Dang YH, Cai J, Li X, Wang L, Li F. Imaging potential and biodistribution in vivo of 2-[18F]fluoropropionic acid in breast cancer-bearing mice. *Zhongguo Yi Xue Ke Xue Yuan Xue Bao*. 2015;37(3):320–324. doi:10.3881/j.issn.1000-503X.2015.03.014.
12. Pillarsetty N, Punzalan B, Larson SM. 2-^{18}F-fluoropropionic acid as a PET imaging agent for prostate cancer. *J Nucl Med*. 2009; 50(10):1709–1714. doi:10.2967/jnumed.109.064212.
13. Wang HL, Hu KZ, Tang GH, Tingting H, Xiang L. Simple and efficient automated radiosynthesis of 2-18F-fluoropropionic acid using solid-phase extraction cartridges purification. *J Label Compd Radiopharm*. 2012;55(9):366–370. doi:10.1002/jlcr.2952.
14. Li L, Che L, Tharp KM, et al. Differential requirement for de novo lipogenesis in cholangiocarcinoma and hepatocellular carcinoma of mice and humans. *Hepatology*. 2016;63(6):1900–1913. doi:10.1002/hep.28508.
15. Fakhri GE. Ready for prime time? Dual tracer PET and SPECT imaging. *Am J Nucl Med Mol Imaging*. 2012;2(4):415–417.
16. Vavere AL, Kridel SJ, Wheeler FB, Lewis JS. 1-11C-acetate as a PET radiopharmaceutical for imaging fatty acid synthase expression in prostate cancer. *J Nucl Med*. 2008; 49(2): 327–334. doi:10.2967/jnumed.107.046672.
17. Buchanan JM, Hastings AB, Nesbett FB. The role of carboxyl-labeled acetic, propionic and butyric acids in liver glycogen formation. *J Biol Chem*. 1943;150:413–425.
18. Ricks CA, Cook RM. Regulation of volatile fatty acid uptake by mitochondrial acyl CoA synthetases of bovine liver. *J Dairy Sci*. 1981;64(12):2324–2335. doi:10.3168/jds.S0022-0302(81)82854-8.
19. Cao D, Song X, Che L, et al. Both de novo synthetized and exogenous fatty acids support the growth of hepatocellular carcinoma cells. *Liver Int*. 2017;37(1):80–89. doi:10.1111/liv.13183.
20. Wehrle JP, Ng CE, McGovern KA, et al. Metabolism of alternative substrates and the bioenergetic status of EMT6 tumor cell spheroids. *NMR Biomed*. 2000;13(6):349–360.
21. Malaisse WJ, Zhang TM, Verbruggen I, Willem R. Enzyme-to-enzyme channelling of Krebs cycle metabolic intermediates in Caco-2 cells exposed to [2-13C]propionate. *Biochem J*. 1996; 317(Pt 3):861–863.
22. Wysham WZ, Roque DR, Han J, et al. Effects of fatty acid synthase inhibition by orlistat on proliferation of endometrial cancer cell lines. *Target Oncol*. 2016;11(6):763–769. doi:10.1007/s11523-016-0442-9.
23. Wang C, Xu C, Sun M, Luo D, Liao DF, Cao D. Acetyl-CoA carboxylase-alpha inhibitor TOFA induces human cancer cell apoptosis. *Biochem Biophys Res Commun*. 2009;385(3): 302–306. doi:10.1016/j.bbrc.2009.05.045.
24. Li S, Qiu L, Wu B, et al. TOFA suppresses ovarian cancer cell growth in vitro and in vivo. *Mol Med Rep*. 2013;8(2):373–378. doi:10.3892/mmr.2013.1505.
25. Heo CK, Woo MK, Yu DY, et al. Identification of autoantibody against fatty acid synthase in hepatocellular carcinoma mouse model and its application to diagnosis of HCC. *Int J Oncol*. 2010;36(6):1453–1459.
26. Menendez JA, Lupu R. Fatty acid synthase and the lipogenic phenotype in cancer pathogenesis. *Nat Rev Cancer*. 2007;7(10): 763–777. doi:10.1038/nrc2222.
27. Wang B, Ding YM, Fan P, Wang B, Xu JH, Wang WX. Expression and significance of MMP2 and HIF-1alpha in hepatocellular carcinoma. *Oncol Lett*. 2014;8(2):539–546. doi:10.3892/ol.2014.2189.